ELSEVIER

Journal of Power Sources 97–98 (2001) 726–732

JOURNAL OF POWER SOURCES

www.elsevier.com/locate/jpowsour

Cooperative research on safety fundamentals of lithium batteries

J. Robert Selman[a,*], Said Al Hallaj[a], Isamu Uchida[b], Y. Hirano[b]

[a]*Illinois Institute of Technology (IIT), Center for Electrochemical Science and Engineering (CESE), 10 West 33rd Street, Chicago, IL 60616, USA*
[b]*Department of Applied Chemistry, Graduate School of Engineering, Tohoku University, 07 Aramaki Aoba, Aoba-ku Sendai 980-8579, Japan*

Received 1 June 2000; received in revised form 20 January 2001; accepted 22 January 2001

Abstract

A cooperative research program on the thermal characterization and safety of lithium batteries is being carried out at IIT/Center for Electrochemical Science and Engineering and Tohoku University. This research includes experimental work for commercial lithium secondary batteries and performance prediction for scaled-up batteries. In this work, we present a set of thermal characterization experiments for lithium secondary battery cells under normal and abuse conditions. These show that the rise in cell temperature depends strongly on cell chemistry as well as discharge rate. Computer simulation of the cycling of scaled-up lithium batteries shows that the cell temperature profile also depends strongly on the surface cooling rate. An effective thermal management system is required to operate these batteries safely. This paper reviews the basic information needed for intrinsically safe design. © 2001 Elsevier Science B.V. All rights reserved.

Keywords: Lithium batteries; Thermal run-away; Entropy effect; Scale-up design

1. Introduction

The primary challenge in designing a scaled-up lithium battery system is safety under abusive as well as normal operating conditions. During battery charge/discharge, various chemical and electrochemical reactions as well as transport processes take place. Some of these reactions and processes continue also under open circuit conditions. They are largely exothermic and may cause battery temperature to rise if the rate of heat transfer from the battery to the surroundings is not sufficient. This may be the case if the battery is operated under insulating conditions or in a hot environment. It will cause battery temperature to rise significantly, and ''hot spots'' may form within individual cells. Such hot spots are likely to accelerate and spread local heat evolution, thereby leading to thermal run-away. Even in the absence of hot spots, excessive overall temperature rise is likely to cause rapid capacity fading.

Quantitative measurements of the heat generation rate inside the battery during normal and abuse conditions are important to design and develop a suitable thermal management system for scaled-up battery systems. Such measurements can be obtained using the accelerated rate calorimeter (ARC).

In previous work using electrochemical–calorimetric measurements, the IIT group has measured heat generation rates under different charge/discharge rates for a few commercial lithium-ion batteries [1–3]. The measured heat generation and thermo-physical properties were incorporated later in a thermal model to design and simulate the performance of scaled-up lithium-ion cells of 10–100 Ah which are suitable for EV application [4]. Preliminary results indicated that the temperature increase in the scaled-up cells is a major concern when the cells are operated at high discharge rates or under natural convection cooling conditions.

In our cooperative research project, the heat dissipation rates of a number of cells during charge/discharge were measured. This paper presents an overview of results for commercial cells with different designs and chemistries.

2. Strategy

2.1. ''Normal operation'', and effects associated with ''abnormal'' operation

Lithium-ion battery manufacturers tend to be very conservative in setting the upper limit on the ''normal''

* Corresponding author. Tel.: +1-312-567-3037; fax: +1-312-567-6914.
E-mail address: selman@iit.edu (J.R. Selman).

PII: S0378-7753(01)00732-7

operating temperature, for example, 65°C for Sony US type 18650 lithium cobaltate cells. This is to avoid excessive capacity fading as well as thermal run-away. The mechanisms of these processes are complicated and both are poorly predictable but the likelihood of their occurrence increases rapidly with temperature. During discharge, the risk of thermal run-away is increased due to the combined exothermic effects of chemical reaction and resistive heating.

Thus, it is obvious that thermal run-away occurs due to a superposition of ''normal-use'' heat effects and ''abnormal'' heat effects caused by physical transformations of cell materials, or chemical reactions between them. These transformations and reactions are always going on, even during normal use, and they are responsible for capacity fading. However, both capacity fading and the risk of thermal run-away are accelerated when the ''normal'' processes, operating at the margin of the safety range for cell temperature and current level, generate increasingly high temperatures and ''hot spots''. One objective of our strategy is to determine the ''abnormal'' heat effects and the chemical reactions responsible for them. This may be done by well-controlled experiments, using the ARC. In these experiments, the overall heat generation is accurately measured, and the ''abnormal'' heat effect backed out by subtraction of the ''normal'' heat effects.

2.2. Sources of heat generation and their effect on cell performance/thermal run-away

Three sources of heat generation must be considered in the analysis of capacity fading and thermal run-away:

1. The ''reversible'' heat released (or absorbed) by the chemical reaction of the cell.
2. The ''irreversible'' heat generated by ohmic resistance and polarization.
3. The heat generated by ''side reactions'', i.e. parasitic/corrosion reactions, and ''chemical shorts''.

In ''normal operation'', heat effects (1) and (2) are small. Therefore, no thermal run-away occurs even during prolonged operation, and capacity fading is not accelerated. However, the heat generation rate due to chemical reaction increases linearly with the level of the current, and the rate of resistive heating increases quadratically with current load. Therefore, under abusive conditions, i.e. excessive loads (high discharge current) and accidental shorts, heat effects (1) and (2) cause high overall temperature. This is made worse by operation at the margin of the safe temperature range. Such an ''abnormal operation'' is likely to generate a very non-uniform temperature distribution (including ''hot spots''). The high overall temperature accelerates uniform degradation of active materials, thereby degrading cell performance and cycle life. The hot spots may accelerate heat effect (3) to the point where thermal run-away is triggered.

2.3. Experimental determination of the ''abnormal'' heat effect

From thermal run-away experiments on small cells at open circuit it is possible to extract information about heat effect (3), including the activation energy of the degradation reactions [5]. Such information is indispensable for models of the thermal run-away process [6,7], which must be based on assumptions concerning specific chemical reactions taking place. However, the interaction between the ''normal use'' heat effects, which continue to operate in the ''abnormal use'' range, and the degradation reactions which trigger the thermal run-away reaction remains unclear. Practically, useful models of the thermal run-away process must include a superposition of ''normal'' and ''abnormal'' heat effects, which may be fitted by experimental data.

2.4. Heat generation under ''normal'' conditions

From the above, it is clear that the ''normal use'' heat effects must be accurately known to allow determination of the heat effect (3). In our work, we have found that especially the reversible heat effect (1) must be accurately known, since it is the dominating heat effect in the discharge of most lithium-ion batteries (see Section 3.4).

The reversible heat of a cell may be measured calorimetrically by various techniques [2,3] or may be calculated from the temperature dependence of the equilibrium potential of the cell, using the thermodynamic equation:

$$Q_{\mathrm{rev}} = n_{\mathrm{Li}} T \Delta S = T\left(\frac{\partial E_{\mathrm{eq}}}{\partial T}\right)(It)_{\mathrm{dc}}$$

In the first phase of this cooperative research, we have determined the entropy coefficient for various lithium cells under ''normal'' operating conditions.

2.5. Model for thermal run-away and accelerated capacity fading

In the ongoing second phase, we are developing a practical model for thermal run-away and capacity fading, based on thermal run-away at open circuit and under load, using ARC measurements. A few representative measurements are reported here.

3. Results and discussion

In the following, techniques used to implement this strategy are illustrated, and important results highlighted. Details may be found in the referenced publications.

3.1. Measurement of overall heat effect during cycling

The ARC-battery cycler experimental set-up was used to measure the temperature, voltage and current of the cells at

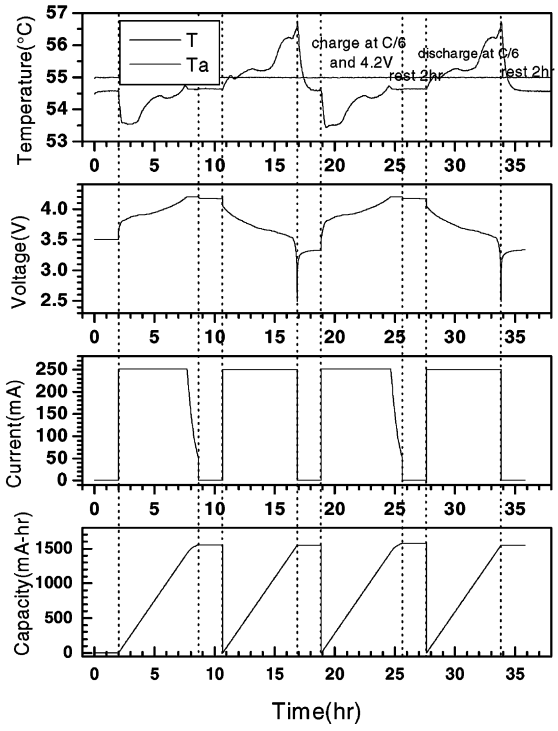

Fig. 1. Temperature/voltage/current/capacity profile during cycling of a Panasonic lithium-ion cell ($LiCoO_2$/graphite) at C/6, T(ambient) = 55°C.

different charge/discharge rates. Fig. 1 shows measurements taken for a Panasonic type 18650 cell ($LiCoO_2$/graphite) at C/6 charge/discharge rate and an operating temperature of 55°C. As reported earlier [1–4], the cell showed good cyclability with a net cooling effect during charge and a highly exothermic effect during discharge.

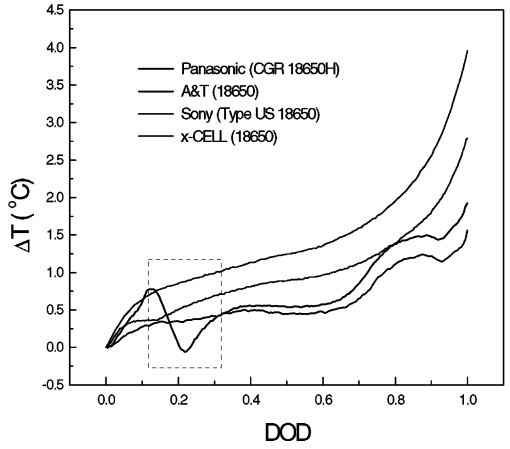

Fig. 2. Temperature profiles during discharge of different commercial type 18650 lithium-ion cells at C/6 rate and T(ambient) = 35°C.

Fig. 2 shows cell temperature measurements for Sony (type US18650), Panasonic (type CGR 18650H), A&T (type 18650), and x-18650 cells, during discharge at C/6 rate. The x-18650 cell has graphite and $LiCo_{0.2}Ni_{0.8}O_2$ as anode and cathode materials, respectively. Panasonic (CGR 18650H), Sony (type US 18650) and A&T (type 18650) cells have Li_x-CoO_2 as cathode material. The Panasonic cell (CGR 18650H) has a graphite anode, while the Sony (type US18650) and A&T (type 18650) cells have hard carbon and graphitized carbon fiber, respectively, as anode materials [2,6].

3.2. Measurement of reversible (or entropic) heat effect

The Panasonic cell showed an unexpected cooling effect near DOD = 0.2. This was related to the unexpected strong

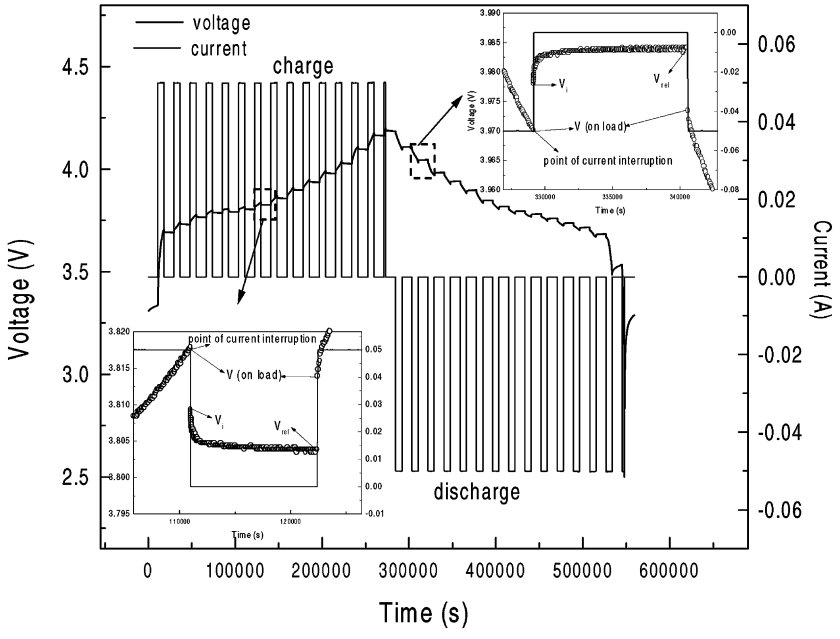

Fig. 3. dc Impedance measurement by current interruption during charge/discharge of a type 18650 lithium-ion cell (schematic).

variation of the entropy heat effect due to the near-simultaneous occurrence of a phase change in the cathode and a structural transformation (quasi-phase change) in the graphite anode. The entropic heat effect was measured using dc-current interruption in combination with calorimetric measurements (DCIC) during charge and discharge of the cell, as shown in Fig. 3 [2].

3.3. Entropic heat effect during charge/discharge, and contributions of PE and NE

Fig. 4 shows entropy coefficient (dE_{eq}/dT) measurements for different commercial cells at different states of charge (SOC). The negative values for dE_{eq}/dT indicate that the entropic heat generation is endothermic during charge and exothermic during discharge.

In addition, entropy coefficients were obtained for coin cells having a lithium-ion electrode material as one electrode and lithium metal as the opposite electrode

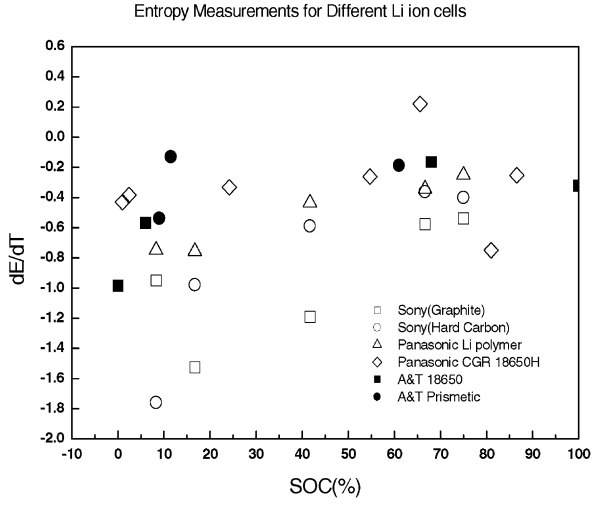

Fig. 4. Entropy coefficients of commercial secondary lithium batteries as a function of state-of-charge.

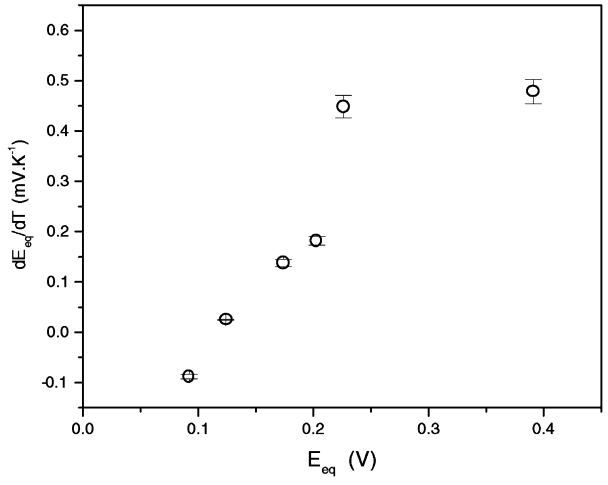

Fig. 5. Entropy coefficient of a graphite/Li half-cell as a function of OCV.

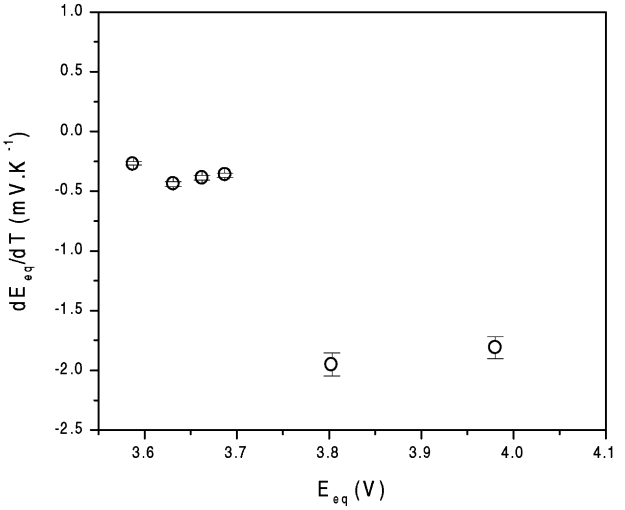

Fig. 6. Entropy coefficient of a $LiNi_{0.8}Co_{0.2}O_2$/Li half-cell as a function of OCV.

(“half-cells”). As shown in Figs. 5 and 6 for graphite and $LiNi_{0.8}Co_{0.2}$ O_2, respectively, the entropic effect of half-cells having cathode materials is similar to that found for the whole cell, while the graphite half-cell has an opposite effect, i.e. exothermic during charge and endothermic during discharge.

3.4. Dominant contribution of the heat effect in lithium-ion cells

Based on these and other measurements [3], calculations illustrated in Fig. 7 show that entropic heating accounts for more than 50% of the total heat generated during discharge in cobaltate based lithium-ion cells, when discharged at high rate (i.e. C/1 and C/2), and over 60% at low discharge rates (i.e. C/3 and C/6). However, the amount of heat generated is strongly dependent on the discharge rate and the chemistry of the cell materials.

3.5. Temperature profiles in scaled-up lithium-ion cells

The data base on heat-generation rates determined from measurements such as Figs. 1–3 allows us to calculate temperature profiles in individual battery cells, as well as battery packs. Under “normal-use” conditions, a simplified one-dimensional thermal mathematical model with lumped parameters may be used to predict the temperature profiles [1]. This model was used to simulate temperature profiles under different operating conditions and cooling rates for scaled-up cylindrical lithium-ion cells of 10 and 100 Ah capacity. Figs. 8 and 9 illustrate that, as expected, the cooling rate has a strong effect on cell temperature for all discharge rates. However, the temperature gradient is not significantly affected by the cooling rate except at very high rates (Biot number > 0.1). At cooling rates typical of passive cooling systems, the temperature distribution

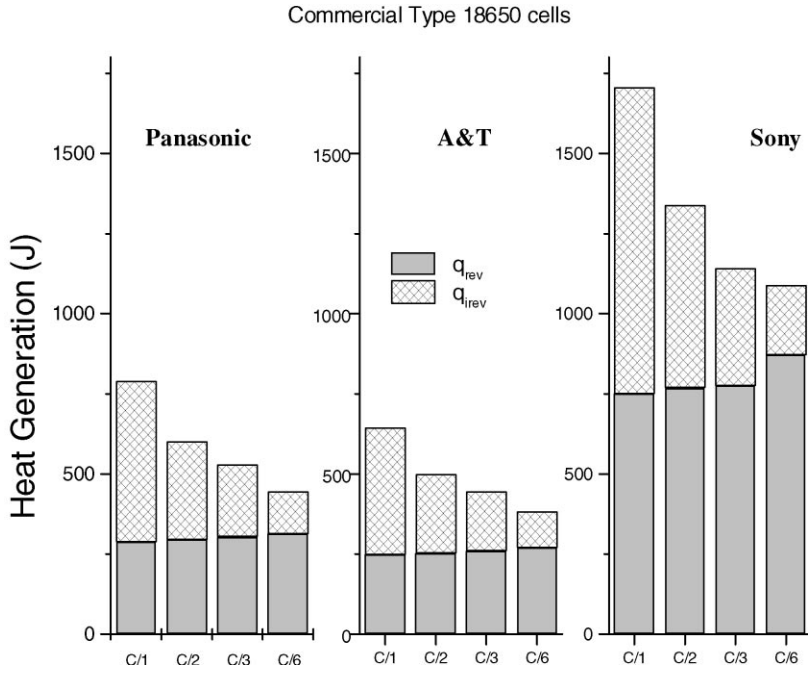

Fig. 7. Contributions of reversible and irreversible heat to total heat generation for a cobaltate-based type 18650 lithium-ion cell, at different discharge rates.

remains by large uniform, so that the assumption of lumped heat generation parameters for the cell as a whole is justified.

3.6. The ARC measurements of thermal run-away

To elucidate the mechanism of performance degradation and thermal run-away, it is helpful first to study these processes experimentally at open circuit. For example, using an ARC it was established earlier that thermal run-away at open-circuit is sensitive to the state-of-charge. Using Sony type 18650 cells, it was found to occur at 104°C for cells charged to 4.06 V open circuit, and at 144°C for cells at 2.8 V open circuit [4]. A similar measurement of thermal run-away at open circuit, using a small prismatic cell at 3.52 V, is shown in Fig. 10. It can be seen that, clearly, there are two trigger temperatures, one of which is the conventional run-away temperature (in this case, 96.7°C). However,

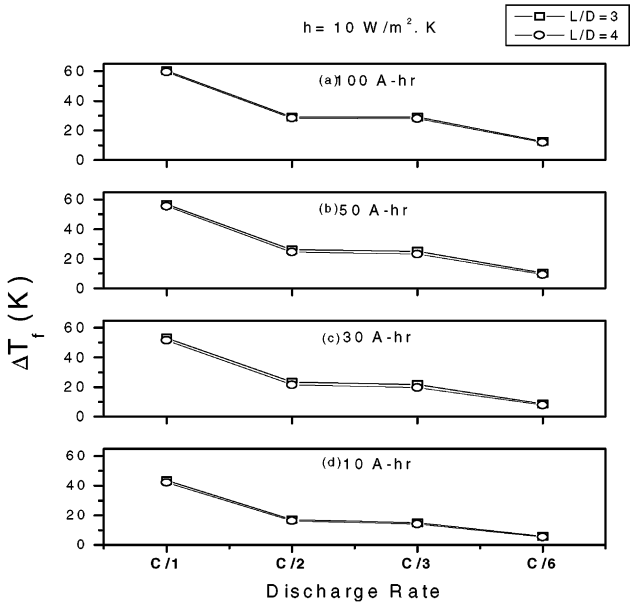

Fig. 8. Predicted temperature profiles for scaled-up lithium-ion batteries at different discharge rates under natural-convection cooling conditions, $h = 10$ W/(m^2 K).

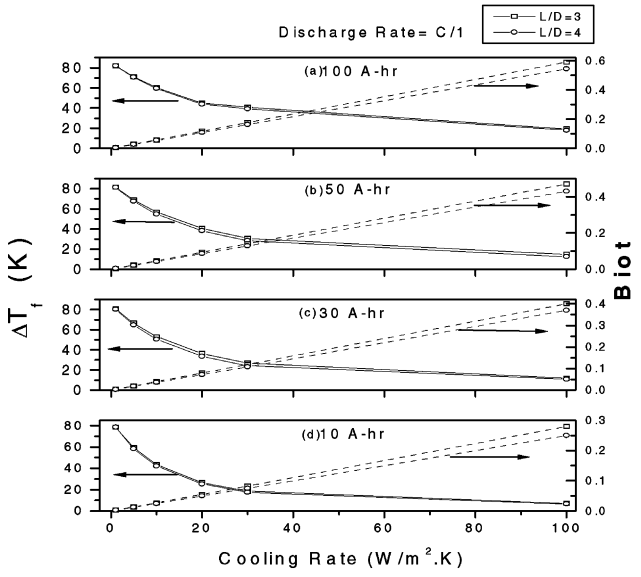

Fig. 9. Effect of cooling rate on the temperature increase of scaled-up lithium-ion batteries at C/1 discharge rate.

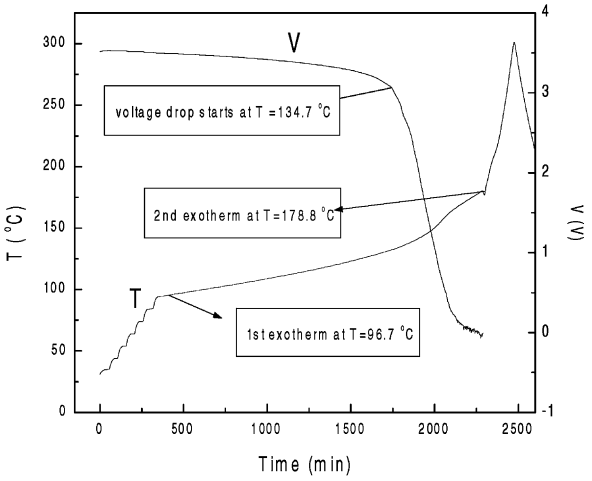

Fig. 10. Temperature and voltage profiles during thermal run-away testing (using ARC) of a 550 mAh prismatic A&T cell at 3.52 V open-circuit voltage.

cell voltage is not affected much until 134.7°C and a second, much more significant exotherm, starts at 134.7°C. Although this type of experiments yields primary information about trigger temperatures and activation energies, the information is not sufficient as the basis for a comprehensive model. The heat-effect information is not consistent from one experiment to another, even for the same cell type. Even the run-away temperature (or trigger temperatures) may differ from one experiment to another depending on the ''history'' of the cell and the load.

As a first step to supplement the information obtainable from such experimental data and understand their variability, we apply various diagnostics during the thermal run-away experiment [8]. As shown in Fig. 11, ac impedance measurements are useful to identify the events or reactions occurring at various points in the run-away process.

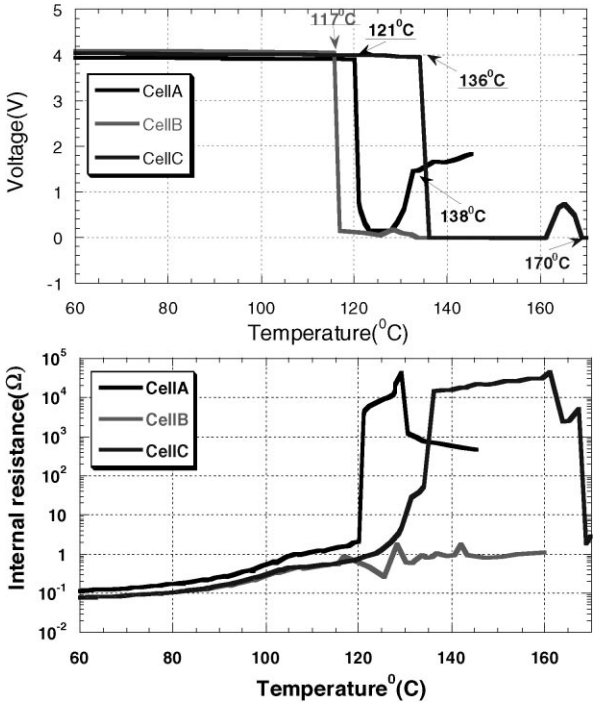

Fig. 11. The voltage and the internal resistance profile of the cell in thermal run-away experiment (ac impedance calorimetric). Cell A: $E = 3.94$ V, SOC = 75%; cell B: $E = 4.11$ V, SOC = 75%; cell C: $E = 4.05$ V, SOC = 75%.

4. Conclusions

We have demonstrated that a systematic approach to understanding the safety fundamentals of lithium-ion cells helps to develop practically useful models. In the work presented here, we have emphasized the thermal run-away process but the approach is equally applicable to capacity fading. A key requirement is accurate information about the reversible heat effect of the lithium-ion cell, which is specific for the cell chemistry and dominates the overall heat effect in ''normal use''.

To unravel the mechanism triggering run-away, the ''normal use'' heat effect may be combined to predict temperature profiles in a cell of arbitrary size, under any operating conditions. This allows one to develop models for thermal run-away. One way to model the run-away process is to take a critical (triggering) temperature for granted (as determined by ARC experiments) and to fit experimental heat release data to yield a generalized heat effect. The latter may then be interpreted in terms of specific degrading reactions. Alternatively, one may hypothesize certain degrading reactions (specific for each cell component) with well-known heats of reaction. The model then would be fitted to experimental data to produce critical temperatures (or more likely, critical temperature ranges) in which acceleration of the degrading reactions takes place, corresponding to trigger points in the run-away process.

Acknowledgements

Work at IIT was supported by the Army Research Office under Grant No. DAAH 04-94G-0055 and the Office of Naval Research under equipment Grant 5-57672, no. ARO DAAH 04-95-1-0569 (1995–2000). Work at Tohoku University was supported by the Ministry of Education via NICHe.

References

[1] S. Al Hallaj, J. Prakash, J.R. Selman, J. Power Sources 87 (2000) 186–194.
[2] S. Al Hallaj, J. Prakash, J.R. Selman, J. Electrochem. Soc. 147 (2000) 2432–2436.

[3] J.S. Hong, H. Maleki, S. Al Hallaj, L. Redey, J.R. Selman, J. Electrochem. Soc. 145 (1998) 1489–1501.
[4] S. Al Hallaj, J.S. Hong, H. Maleki, J.R. Selman, J. Power Sources 83 (1999) 1–8.
[5] S. Al Hallaj, Y. Hirano, T. Itoh, T. Abe, J.R. Selman, I. Uchida, in: Proceedings of the International Lithium Battery Workshop, Kyoto, Japan, 14–17 November 1999.
[6] B.A. Johnson, R.E. White, J. Power Sources 70 (1998) 48–54.
[7] L. Rao, J. Newman, J. Electrochem. Soc. 144 (1997) 2697–2704.
[8] Y. Hirano, M. Mohamedi, Y. Hisamitsu, T. Itoh, M. Umeda, I. Uchida, in: Proceedings of the Japan Battery Symposium on ac Impedance Measurements of Lithium-Ion Cells in ARC, Nagoya, Japan, 20–22 November 2000.